

SOURCE LOCALIZATION BY DIFFRACTION STACKING

D. Anikiev, D. Gajewski, B. Kashtan, E. Tessmer and C. Vanelle

email: *dirk.gajewski@zmaw.de*

keywords: *Source localization, diffraction stack, autocorrelation*

ABSTRACT

The localization of seismic events is not only of great importance in seismology but also in exploration seismics for hydro frac and reservoir monitoring. We introduce a new localization technique which does not require any picking of events in the individual seismograms of the recording network. The localization is performed by a modified diffraction stack of autocorrelated seismograms to obtain the source location. Numerical results for 2-D homogeneous media indicate, that the method provides very good results if the velocity model is correct. For this case we show that the maximum amplitude of the stacking process occurs at the exact location of the source. Numerical examples reveal that satisfactory results are obtained with the stacking procedure even if the velocity model is not precisely known.

INTRODUCTION

The problem of earthquake location is one of the most basic problems in seismology. It is stated as follows (Pujol, 2004): Given a set of arrival times and a velocity model, determine the origin time and the coordinates of the hypocenter of the event. This definition inherently assumes that the arrivals of an event are visible on a certain number of stations of the observing array. It also means, that the arrival has to be identified in the seismogram prior to the actual localization of the event. This not only requires the correct identification of the onset of the arrivals but also the proper correlation of the event among the different stations of the network.

Source location methods are categorized into absolute location methods and relative location methods. For the first type, the determination of the excitation time and hypocenter of a seismic source is traditionally performed by minimizing the difference between the observed and predicted arrival times of the seismic event. For recent advances in seismic event location using such approaches see, e.g., Thurber and Rabinowitz (2000). The second class of methods considers relative location within a cluster of events using travel time differences between pairs of events or stations, see, e.g., Waldhauser and Ellsworth (2000). These methods allow improvement of the relative location between seismic sources but are exposed to the same difficulties mentioned above. For all mentioned techniques, it is assumed that the event is visible on at least a few stations of the recording array.

Recently, Gajewski and Tessmer (2005) introduced a localization method based on reverse modeling (back projection with time reversal) which does not require any picking of events. Another advantage of this method is the focussing of energy in the back projection process which allows to image very weak events which could not be identified in the individual seismogram of the recording network.

Back projection can also be performed by stacking of amplitudes of seismic traces. We will first introduce the methodology of the stacking approach which is different to stacking seismic reflection data since the excitation time of the source is not known. Numerical 2-D examples using the correct and erroneous velocities illustrate the capabilities of the suggested approach.

METHODOLOGY

In a passive seismic experiment, the seismic network records all seismic events emitted during a certain time periode. The start of the recording is denoted by t_1 and the end of the recording is t_2 . The excitation time of the event as well as the location in the subsurface are initially not known. Here, we consider acoustic emissions with small magnitude, i.e., point source events. The spatial extent of the fault plane for these events is small compared to the prevailing wavelength of the recorded signal.

For the event location we first discretize the subsurface. The discretization should be small enough to achieve the required location accuracy which is also limited by the bandwidth of the event under consideration (see, e.g., Gajewski and Tessmer (2005)). The chosen area limits the space where events can be located. The number of receivers, the receiver spacing and the aperture are given by the acquisition geometry of the passive seismic experiment. Here we consider 2-D examples and the seismic networks are linear equally spaced surface arrays. The receiver coordinate is specified by ξ and the aperture is $2L$.

Source location

Every point of the discretized subsurface is considered as a potential source position. First we consider a homogeneous medium and assume that the velocity is known prior to localization. For this case travel-times $\tau(\xi; x, z)$ at the surface location ξ for each subsurface location (x, z) are uniquely defined and are obtained analytically. The recorded seismograms for the time window from t_1 to t_2 serve as input data. The amplitudes of each trace are stacked along the diffraction traveltime curve for the subsurface point (x, z) under consideration. If the traveltime is between two samples of the seismogram, amplitudes may be interpolated. Since we do not know the excitation time of the source the stack needs to be performed for any possible origin time T within the recorded time window leading to $(t_2 - t_1)/\Delta t$ stacks for this particular location. This means, we are shifting the traveltime curve through the recorded time window and stack for each time step. Finally the amplitudes of the stack are squared and summed for all considered times. The result comprises the value of the so called image function IM for the position (x, z) . This procedure is repeated for all possible subsurface locations (loops over all possible x and z) which leads to a section of the image function. The source location is obtained by searching the maximum of the image function $IM(x, z)$.

If we assume that the amplitudes of the seismic traces are constant (e.g., by normalization in the time window under consideration) we can formally describe this process and investigate the image function analytically. The seismic trace with the seismic event is expressed by the high frequency representation,

$$u(\xi, t) = Af[t - \tau_0(\xi; x_0, z_0)],$$

where A is the constant Amplitude (assumed to be unity in the following) and $\tau_0(\xi; x_0, z_0)$ is the travel time for the event generated by the source at position (x_0, z_0) and recorded at location $(\xi, 0)$ at the recording surface. We perform the stack along the diffraction time $\tau(\xi; x, z)$ over the whole aperture $2L$ for a time $t = T + \tau(\xi; x, z)$ where T corresponds to a time within the recording window from t_1 to t_2 . The diffraction time $\tau(\xi; x, z)$ corresponds to the traveltime from location $(\xi; x, z)$ to the receivers at ξ . This process is formally described by

$$W(T, x, z; x_0, z_0) = \int_{-L}^L f[\xi, T + \tau(\xi; x, z) - \tau_0(\xi; x_0, z_0)] d\xi. \quad (1)$$

According to the description of the previous paragraph, the image function at (x, z) is obtained by squaring and adding the results of Eq. 1 for each time step over the whole recording window leading to the integral

$$IM(x, z) = \int_{t_1}^{t_2} W^2(T, x, z; x_0, z_0) dT. \quad (2)$$

Finally, the source location is determined by searching the maximum of the image function (Eq. 2), i.e.,

$$\max (IM(x, z)) = IM(x_0, z_0).$$

In the next section we will investigate the image function in some more detail and we show that for a correct velocity model the location of the maximum of the image function in fact corresponds to the source location.

Properties of the image function

We consider the Fourier transform of a signal f , i.e.,

$$f[\xi, T + \tau(\xi; x, z) - \tau_0(\xi, x_0, z_0)] = \int_{-\infty}^{\infty} F(\omega) e^{i\omega(\tau(\xi, x, z) - \tau_0(\xi, x_0, z_0) + T)} d\omega \quad ,$$

where $F(\omega)$ is the spectrum of the event and ω is frequency. Using this expression the stack integral (Eq. 1) reads:

$$W(T, x, z; x_0, z_0) = \int_{-L}^L d\xi \int_{-\infty}^{\infty} F(\omega) e^{i\omega(\tau(\xi, x, z) - \tau_0(\xi, x_0, z_0) + T)} d\omega \quad (3)$$

Let us now introduce a function S according to the relation

$$S(\omega, x, z; x_0, z_0) = \int_{-L}^L e^{i\omega[\tau(\xi, x, z) - \tau_0(\xi, x_0, z_0)]} d\xi \quad (4)$$

which allows to rewrite the stack integral (Eq. 3) in the following form:

$$W(T, x, z; x_0, z_0) = \int_{-\infty}^{\infty} F(\omega) S(\omega, x, z; x_0, z_0) e^{i\omega T} d\omega.$$

The image function is obtained by squaring the stacked result W and integration over the recording time window. Since we can always add zeroes to the signal (zero padding) we will perform the time integration without limits, i.e.,

$$IM(x, z; x_0, z_0) = \int_{-\infty}^{\infty} W^2(T, x, z; x_0, z_0) dT = \frac{1}{2\pi} \int_{-\infty}^{\infty} |F(\omega)|^2 |S(\omega, x, z; x_0, z_0)|^2 d\omega \quad , \quad (5)$$

where we have applied Parseval's theorem to obtain the last equality. Obviously, function S has a maximum when the traveltimes $\tau(\xi, x, z)$ and $\tau_0(\xi, x_0, z_0)$ coincide. For the correct velocity model this leads to the condition $x = x_0$ and $z = z_0$ and

$$\max(|S(\omega, x, z; x_0, z_0)|) = |S(\omega, x_0, z_0; x_0, z_0)| \quad ,$$

i.e., the maximum of function S is obtained, if the considered subsurface point coincides with the actual source position at (x_0, z_0) . The same applies to the location of the maximum of the image function IM . Moreover, the image function at the source location corresponds to the sum of the autocorrelation of each recorded trace. A similar result is obtained if we apply the reciprocity principle and time reversal as used in the reverse modeling approach by Gajewski and Tessmer (2005).

The above procedure allows to determine the source position from the data without picking. Due to the stacking of energy (squared amplitudes) involved in this procedure even small events not visible in a single seismic trace may be imaged (see Gajewski and Tessmer (2005)). Another important parameter in the passive seismic method is the excitation time of the event. How this parameter is determined from the data is described in the next section.

Determination of excitation time

To determine the excitation time of a source which was located at a position (\hat{x}, \hat{z}) by the technique described above (corresponding to the exact source coordinates (x_0, z_0) for the homogeneous case), we suggest the following procedure. By evaluating function W^2 (see Eq. 1), i.e., squaring and stacking the amplitudes of the data along the traveltime curve $\tau(\xi, \hat{x}, \hat{z})$ for time T , we obtain one data point $W^2(T, \hat{x}, \hat{z}, x_0, z_0)$. Considering all possible times from $t_1 \leq t \leq t_2$ we obtain a time series of N points for function $W^2(t, \hat{x}, \hat{z}, x_0, z_0)$. The excitation time t_0 is given by the maximum of this function, i.e., at the time where the maximum amplitude of this time series is observed:

$$\max(W^2(T, \hat{x}, \hat{z}; x_0, z_0)) = W^2(t_0, \hat{x}, \hat{z}; x_0, z_0) \quad .$$

So far we have assumed that the velocity model is known. In the next section we apply techniques based on path integrals to determine the source location with unknown velocity models.

Unknown velocity model

The procedure we suggest here is inspired by path integrals (Feynman and Hibs, 1965) which were recently introduced to seismic migration for imaging without precise velocities (see, e.g., Landa and Moser (2006); Landa (2005, 2004)). Generally we can stack along any kind of trajectory and determine maximum coherency of the results. Here we assume that the stacking trajectories are hyperbolic curves. We allow for varying shapes (i.e., moveouts) of the stacking operator according to different velocity models and stack the results, i.e., we perform an additional integration over the velocities. This leads to a stacked version \hat{S} of the above described function S (see Eq. 4) which reads:

$$\hat{S}(\omega, x, z; x_0, z_0) = \int_{v_1}^{v_2} \int_{-L}^L e^{i\omega[\tau(\xi; x, z) - \tau_0(\xi; x_0, z_0)]} d\xi dv \quad ,$$

where the traveltimes $\tau(\xi; x, z)$ need to be determined for each individual velocity for the velocity v , which varies from v_1 to v_2 for homogeneous models. The image function is obtained in the same way as described in the previous section according to Eq. 4 but using \hat{S} instead of S . Again, the source location is found at the maximum of the image function.

In the next section we present numerical examples for homogeneous models which demonstrate the potential of the procedures and techniques described in this section.

NUMERICAL EXAMPLES

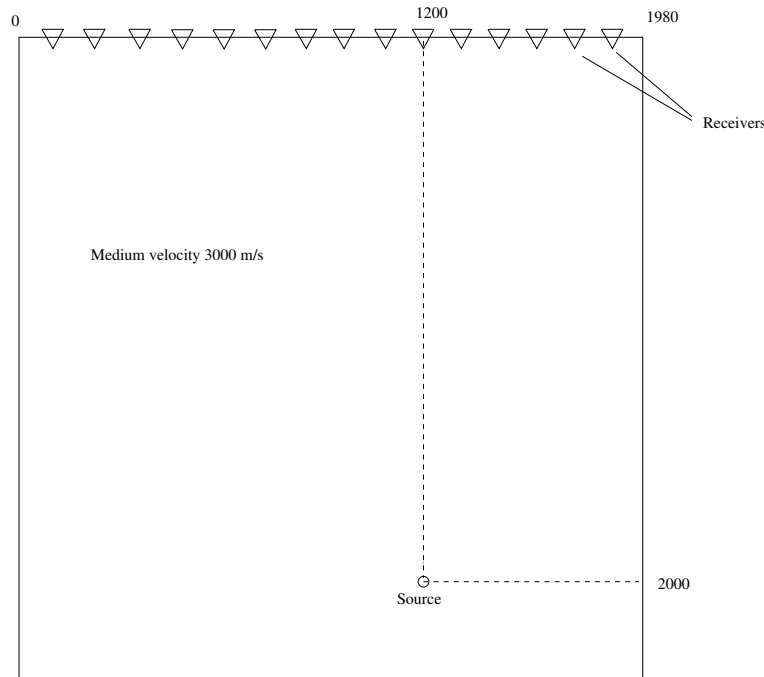


Figure 1: Homogeneous model with $v = 3000$ m/s.

Location with known velocity

In this section the procedure described above is applied to a synthetic data set. The seismograms are generated by a pseudo spectral Fourier modeling code. The model is homogeneous with a velocity of 3 km/s. The grid spacing is 10 m and we consider a total number of 198 receivers. Model and acquisition are displayed in Fig. 1. The seismic source is located at $x=1200$ m and a depth of $z=2000$ m. The location of the source is asymmetric with respect to the center of the recording network. A time-shifted Ricker-wavelet is used in order to simulate a minimum phase wavelet since this best fits real data. The synthetic

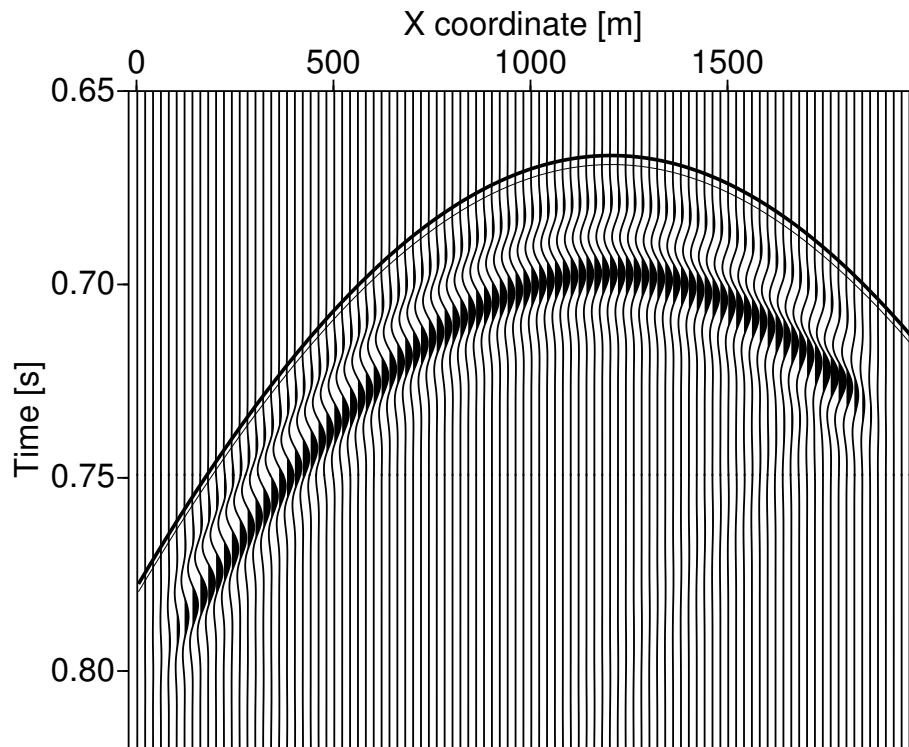


Figure 2: Seismogram with traveltimes curves for the exact source location (thick line) and the position determined by the diffraction stack (thin line) for the signal with 100 Hz prevailing frequency.

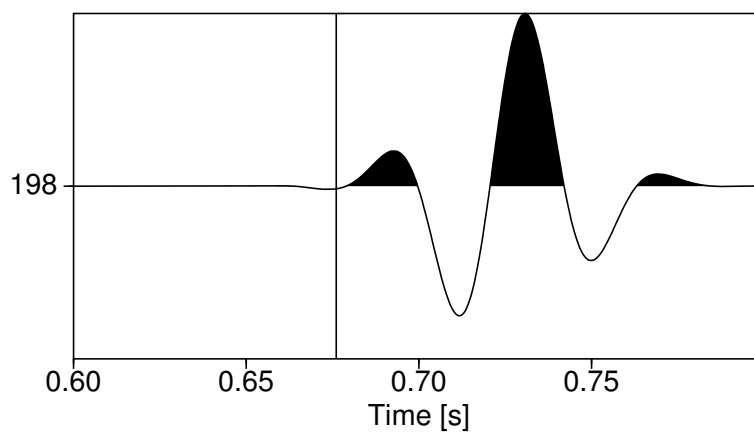


Figure 3: Determined excitation time for a source with 50 Hz prevailing frequency. observed at $x=1200$ m.

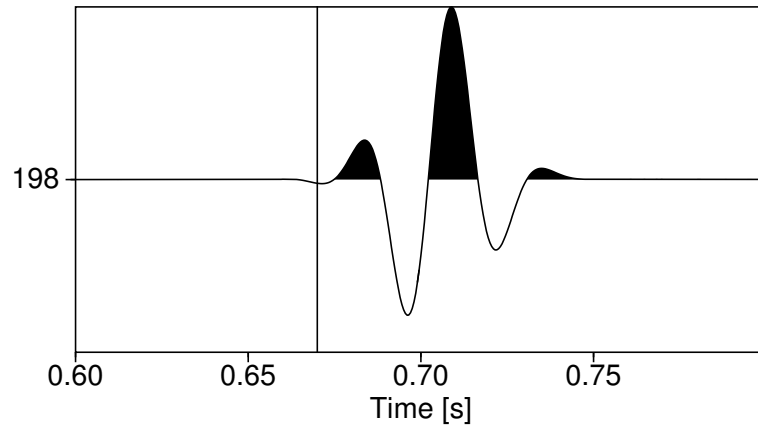


Figure 4: Determined excitation time for a source with 75 Hz prevailing frequency. observed at $x=1200$ m.

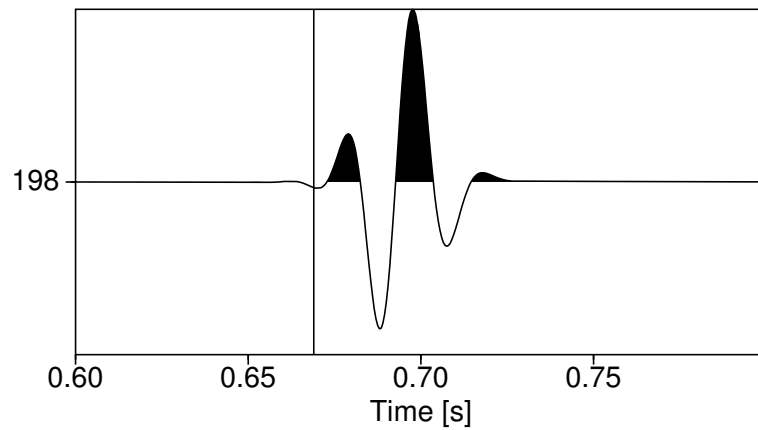


Figure 5: Determined excitation time for a source with 100 Hz prevailing frequency. observed at $x=1200$ m.

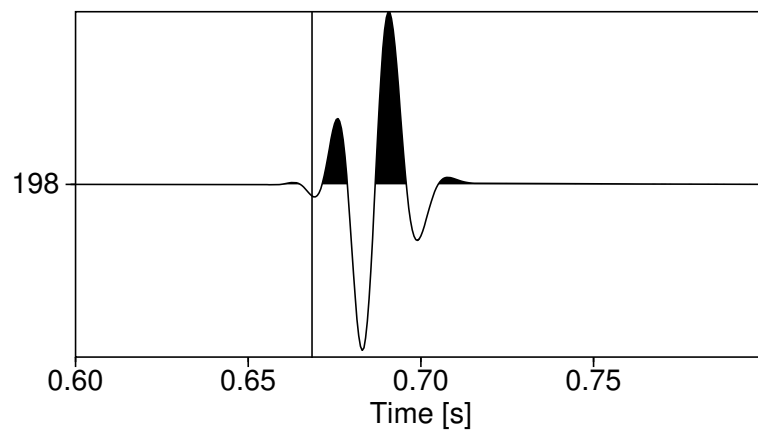


Figure 6: Determined excitation time for a source with 125 Hz prevailing frequency. observed at $x=1200$ m.

Frequency [Hz]	X location error		Z location error	
	Absolute [m]	Relative [%]	Absolute [m]	Relative [%]
25	11.8	1.0	99.4	5.0
50	3.0	0.25	28.2	1.41
75	1.0	0.001	10.0	0.005
100	0.2	0.02	7.0	0.6
125	0.01	0.0001	5.4	0.3

Table 1: Location difference of the maximum of the image function from the exact source location for varying frequencies of the source signal.

seismograms are processed in the above described way to determine source location and excitation time. The discretization of the subsurface used for the diffraction stack to determine the image function is 0.2 m. If the traveltimes for the probed subsurface position is between two samples, the amplitude of the sample closest to the considered traveltimes is used. Since this is a synthetic study the results for the determined source locations are compared with the known values of the modeling

In a first test we investigated the location and timing accuracy with respect to the frequency content of the signal where the correct velocity model is used. The results of the numerical experiments are summarized in Table 1. where signals with prevailing frequencies from 25 to 125 Hz with a frequency step of 25 Hz are considered. The prevailing wavelength for the 125 Hz signal is 24 m. This is already close to the limits of the Fourier modeling of the synthetic data which requires a minimum of 2 samples per shortest wavelength (a 10 m spatial sampling was used for the modelling). We see from Table 1 that the maximum of the image function is closer to the real source position for higher frequencies than for lower frequencies. We observe a continuous increase in the difference of the location of the maximum of the image function from the real source location.

Since the imaging function as described above corresponds to stacking of autocorrelated seismograms, the phase of the signal is removed and has no influence on the stacked result. However, the location where the maximum amplitude of the imaging function is observed depends on frequency. Moreover, the location uncertainty increases with decreasing frequency since the focal area of the image function is wider for lower frequencies than for higher frequencies. The maximum of the image function is located in this focal area and represents the most likely location of the source. Images of the focal area are displayed in the paper by Gajewski and Tessmer (2005).

After the source location is determined we evaluate the excitation time. The combined result of source location and excitation time determination is displayed in Fig. 2 for a source signal with 100 Hz prevailing frequency. Since the determined source location does not perfectly coincide with the exact source location the moveout of the curve representing the traveltimes of the determined location (thin line) does not coincide perfectly with the moveout of the traveltimes curve for the exact location. Due to the location error, also the times do not perfectly coincide. The differences, however, are small. Figs. 3 - 6 display the seismogram at $x=1200$, i.e., above the source location, for prevailing frequencies from 50 to 125 Hz. The determined arrival time is indicated by a vertical line.

So far we have assumed, that the velocity model is known. For a typical reservoir environment this is no limitation since usually reliable velocity models from 3-D seismics and down hole observations are available. If the velocity model is not precisely known we can apply the additional integration over velocities as described above. In the following section we present numerical examples for this case.

Location with unknown velocities

A velocity range from 2.7 km/s to 3.3 km/s is considered, which corresponds to a maximum velocity variation of $\pm 10\%$. A signal with 100 Hz prevailing frequency is used and the spatial discretization for the location procedure with the diffraction stack is again 0.2 m. We first perform the location with the velocities individually without the integration suggested above, i.e., we perform the diffraction stack separately for each velocity starting with 2.7 km/s until 3.3 km/s with a velocity increment of 0.1 km/s.

As expected, the results in Table 2 show that the location accuracy considerably decreases with wrong

Velocity [m/s]	X location error		Z location error	
	Absolute [m]	Relative [%]	Absolute [m]	Relative [%]
2700	34.6	2.9	159.4	8.0
2800	21.0	1.8	91.0	4.6
2900	11.2	0.9	39.4	2.0
3000	0.2	0.02	7.0	0.4
3100	0.2	0.02	65.8	3.3
3200	1.6	0.1	129.4	6.5
3300	1.0	0.08	195.2	9.8

Table 2: Location accuracy for the diffraction stack using different velocity models. The correct velocity is 3000 m/s.

Velocity incr. [m/s]	X location error		Z location error	
	Absolute [m]	Relative [%]	Absolute [m]	Relative [%]
25	6.6	0.6	106.6	5.3
50	6.3	0.5	126.8	6.3
100	7.2	0.6	130.0	6.5
300	6.2	0.5	159.2	8.0

Table 3: Location accuracy for the image functions according to Eq. 4 where different velocity increments were used in the stacks.

velocities. Since we consider homogeneous models and an aperture which is almost symmetrical with respect to the source location the lateral position errors are much smaller than the depth errors. For the maximum velocity variation of -10% we observe a depth error of about 8 % and a lateral location error of about 3%. The increase in error with velocity model difference is non-linear. The lateral location error is smaller for larger velocities than for smaller velocities.

If we additionally perform an integration over velocities by stacking the image functions determined for the different velocities, we obtain a new section. If we search for the maximum amplitude in this section of stacked image functions the location errors as listed in Table 3 are obtained. For a velocity increment of 100 m/s the location accuracy in depth has a relative error of 6.5 % which is better than the values obtained for the individual stacks for 2.7 km/s (8.0 %) and 3.3 km/s (9.8 %). If the velocity increment is decreased to 25 m/s we can improve the location accuracy to 5.3 % by the stack of the image functions. Even if only a rough velocity model is known the summation of all sections determined for the different velocities may lead to an improved location result if compared to a location obtained for a single but wrong velocity.

CONCLUSIONS

We have suggested a new procedure to determine the location of seismic point source events where no picking of arrivals is required. The method is based on the determination of an image function which comprises a stack of autocorrelated seismograms along diffraction curves. It was shown that for homogeneous media the maximum of this image function corresponds to the point source location if the velocity model is known. Numerical examples indicate that the location accuracy depends on the frequency content of the event. The location accuracy considerably decreases if the velocities are not precisely known. The stack over image functions obtained for a range of possible velocities may improve the location accuracy if the exact velocities are not known.

All results may be applied to arbitrary velocity models with vertical and lateral velocity variations. For this case the determination of diffraction traveltimes may require ray tracing. If the velocity is a space dependent function, i.e., $v = v(x, z)$, the integration over v has to be performed for different velocity models.

Surface receiver networks were considered in this study. However, the method is applicable in a similar fashion to downhole networks or a combination of downhole and surface networks. The combined downhole and surface observation considerably improves illumination and should lead to better localization.

The most important part of the stacking procedure is the determination of the traveltimes from the potential source location to the surface or downhole receivers. Very efficient tools are available for this purpose for 2-D and 3-D media which are used for Kirchhoff migration of reflection data. Therefore the extension of the location procedure to 3-D media is straight forward.

ACKNOWLEDGMENTS

We thank the Applied Geophysics Team for helpful discussion. This work was supported by the University of Hamburg, the DAAD (German Academic Exchange Service) and by the sponsors of the *Wave Inversion Technology* (WIT) Consortium.

REFERENCES

- Feynman, R. and Hibbs, A. (1965). *Quantum Mechanics and Path Integrals*. McGraw-Hill Book Co.
- Gajewski, D. and Tessmer, E. (2005). Reverse modelling for seismic event characterization. *Geophys. J. Int.*, 163:276–284.
- Landa, E. (2004). Imaging without a velocity model using path-summation approach. In *Expanded Abstracts*, pages 1016–1019. Soc. Expl. Geophys.
- Landa, E. (2005). Approximate imaging without a precise velocity model: path-summation approach. *Journal of Seismic Exploration*, 14(2-3):235–255.
- Landa, E., F. S. and Moser, T. (2006). Path-integral seismic imaging. *Geophysical prospecting*, 54:1–13.
- Pujol, J. (2004). Earthquake location tutorial: Graphical approach and approximate epicentral location techniques. *Seis. Res. Lett.*, 75(1):63–74.
- Thurber, C. and Rabinowitz, N., editors (2000). *Advances in Seismic Event Location, Modern Approaches in Geophysics*. Geophysical Institute of Israel, Lod.
- Waldhauser, F. and Ellsworth, W. (2000). A double-difference earthquake location algorithm: Method and application to the northern hayward fault. *BSSA*, 90:1353–1368.